Cancer Cell
Article

SYK Inhibition Modulates Distinct PI3K/AKT-Dependent Survival Pathways and Cholesterol Biosynthesis in Diffuse Large B Cell Lymphomas

Linfeng Chen,[1] Stefano Monti,[3,7] Przemyslaw Juszczynski,[1,8] Jing Ouyang,[1] Bjoern Chapuy,[1] Donna Neuberg,[2] John G. Doench,[3] Agata M. Bogusz,[4,9] Thomas M. Habermann,[5] Ahmet Dogan,[6] Thomas E. Witzig,[5] Jeffery L. Kutok,[4,10] Scott J. Rodig,[4] Todd Golub,[3] and Margaret A. Shipp[1,*]

[1]Department of Medical Oncology
[2]Department of Biostatistics
Dana Farber Cancer Institute, Boston, MA 02215, USA
[3]Cancer Program, Broad Institute of MIT and Harvard, Cambridge, MA 02142, USA
[4]Department of Pathology, Brigham and Women's Hospital, Boston, MA 02115, USA
[5]Department of Medicine
[6]Department of Pathology
Mayo Clinic, Rochester, MN 55905, USA
[7]Current address: Section of Computational Biomedicine, Boston University School of Medicine, Boston, MA 02118, USA
[8]Current address: Instytut Hematologii i Transfuzjologii, Poland, Warszawa 02-776
[9]Current address: Department of Pathology, Beth Israel and Deaconess Medical Center, Boston, MA 02215, USA
[10]Current address: Infinity Pharmaceuticals, Cambridge, MA 02139, USA
*Correspondence: margaret_shipp@dfci.harvard.edu
http://dx.doi.org/10.1016/j.ccr.2013.05.002

SUMMARY

B cell receptor (BCR) signaling pathway components represent promising treatment targets in diffuse large B cell lymphoma (DLBCL) and additional B cell tumors. BCR signaling activates spleen tyrosine kinase (SYK) and downstream pathways including PI3K/AKT and NF-κB. In previous studies, chemical SYK blockade selectively decreased BCR signaling and induced apoptosis of BCR-dependent DLBCLs. Herein, we characterize distinct SYK/PI3K-dependent survival pathways in DLBCLs with high or low baseline NF-κB activity including selective repression of the pro-apoptotic HRK protein in NF-κB-low tumors. We also define SYK/PI3K-dependent cholesterol biosynthesis as a feed-forward mechanism of maintaining the integrity of BCRs in lipid rafts in DLBCLs with low or high NF-κB. In addition, *SYK* amplification and *PTEN* deletion are identified as selective genetic alterations in primary "BCR"-type DLBCLs.

INTRODUCTION

Several lines of evidence support the role of B cell receptor (BCR)-mediated survival signals in certain B cell malignancies (Chen et al., 2008; Gupta and DeFranco, 2007; Küppers, 2005; Young et al., 2009). The BCR complex includes membrane-bound immunoglobulin and the disulfide-linked heterodimer, immunoglobulin-α (Igα) and Igβ (also termed CD79A and CD79B, respectively). BCR signaling induces receptor oligomerization and phosphorylation of Igα and Igβ immunoreceptor tyrosine-based activation motifs (ITAMS) by Src family kinases. Following ITAM phosphorylation, the spleen tyrosine kinase (SYK) is recruited and activated, engaging additional adaptor proteins and initiating downstream signaling through phosphatidylinositol-3-kinase (PI3K), NF-κB, extracellular signal-related kinase (ERK)-mitogen-activated protein kinase (MAPK), and NFAT pathways. After ligand binding, BCRs cluster and rapidly associate with cholesterol-enriched membrane microdomains

Significance

Chemical inhibitors of SYK and additional proximal BCR pathway components are in clinical trials in patients with DLBCL and additional B cell malignancies. However, the BCR-dependent survival pathways and respective roles of proximal components such as SYK and PI3K and distal NF-κB signaling remain to be defined. We delineate the downstream signaling, apoptotic, and metabolic pathways perturbed by chemical inhibition or molecular depletion of SYK/PI3K and identify additional genetic bases for enhanced BCR signaling in DLBCLs. These functional and genetic studies further define BCR-dependent DLBCLs and provide a framework for analyzing targeted inhibition of SYK, PI3K, and additional proximal components of the BCR signaling pathway in these tumors.

termed lipid rafts (Dykstra et al., 2003; Gupta and DeFranco, 2007). SYK is recruited to BCR clusters associated with lipid rafts and protein tyrosine phosphorylation is enhanced in these regions (Gupta and DeFranco, 2007).

In addition to ligand-induced receptor aggregation and activation, normal mature B cells rely upon "tonic" BCR-dependent survival signals (Kraus et al., 2004; Monroe, 2006; Srinivasan et al., 2009; Torres et al., 1996). Tonic BCR signaling was initially defined in murine models in which BCR ablation or Igα mutation triggered the apoptosis of normal mature B cells (Kraus et al., 2004; Lam et al., 1997). In follow-up studies, BCR ablation was combined with activation of specific BCR-dependent signaling cascades to delineate the nature of tonic BCR survival signals (Srinivasan et al., 2009). PI3K/AKT signaling, but not NF-κB or MAPK kinase activation, rescued the survival of BCR-deficient B cells (Srinivasan et al., 2009). These studies defined important differences between PI3K/AKT-dependent tonic BCR survival signals and those resulting from activation of additional downstream pathways following BCR engagement (Srinivasan et al., 2009).

Diffuse large B cell lymphomas (DLBCLs) are clinically and genetically heterogeneous disorders in which subsets of tumors share certain molecular features. In the cell-of-origin (COO) classification, groups of DLBCLs share components of their transcriptional profiles with normal B cell subtypes, including germinal center B cells (GC) and activated B cells (ABC) (Wright et al., 2003). In comparison to GC DLBCLs, ABC tumors more frequently exhibit constitutive activation of NF-κB and genetic alterations of several NF-κB pathway components (Compagno et al., 2009; Davis et al., 2001; Rosenwald et al., 2002). This group of DLBCLs is also reported to have more frequent somatic mutations of the Igα or Igβ subunits and altered BCR surface expression, a process termed "chronic active BCR signaling" (Davis et al., 2010). Certain BCR-dependent "ABC" DLBCL cell lines also exhibit constitutive PI3K activation, which modulates downstream NF-κB signaling (Kloo et al., 2011).

Using an alternative approach to define DLBCLs with shared molecular features, we previously applied consensus clustering methods to the transcriptional profiles of primary DLBCLs and identified three highly reproducible tumor groups: BCR, OxPhos (oxidative phosphorylation), and HR (host response) (Monti et al., 2005). "BCR" DLBCLs had increased expression of multiple components of the BCR signaling pathway including SYK (Monti et al., 2005) prompting speculation that these lymphomas relied upon SYK/BCR-mediated survival signals (Chen et al., 2008). This hypothesis was of additional interest given the known role of SYK in tonic BCR signaling (Monroe, 2006) and malignant B cell survival (Chen et al., 2006).

For these reasons, we previously assessed the in vitro efficacy of an ATP-competitive inhibitor of SYK525/526 phosphorylation and activation, R406, in DLBCL cell lines and primary tumors (Chen et al., 2008). Chemical SYK blockade selectively decreased the proliferation and induced apoptosis of surface sIg^+ DLBCL cell lines with intact BCR signaling (Chen et al., 2008). In R406-sensitive DLBCL cell lines, the compound specifically inhibited both baseline- and ligand-induced autophosphorylation of SYK525/526 and SYK-dependent phosphorylation of BCR signaling components such as B cell linker protein BLNK (Chen et al., 2008). The majority of examined sIg^+ primary DLBCLs also exhibited baseline and ligand-induced BCR activity. In these primary tumors, BCR signaling, as reflected by intracellular phospho-BLNK (p-BLNK) expression, was also inhibited by R406 (Chen et al., 2008).

We subsequently performed a clinical trial of the oral SYK inhibitor, fostamatinib (R788), of which R406 is a prodrug, in patients with recurrent B cell non-Hodgkin lymphoma (B-NHL) and found that 22% of patients with DLBCL and 50% of patients with small lymphocytic lymphoma/chronic lymphocytic leukemia responded to treatment (Friedberg et al., 2010). Other investigators also demonstrated the efficacy of chemical inhibition or molecular depletion of SYK in BCR-dependent DLBCL cell lines and in vivo murine lymphoma models (Cheng et al., 2011; Rinaldi et al., 2011; Young et al., 2009). We also recently defined distinct fuel utilization programs in BCR-dependent and BCR-independent/OxPhos DLBCLs (Caro et al., 2012).

Although BCR signaling is an attractive rational therapeutic target and chemical inhibitors of SYK and additional proximal BCR-pathway components have demonstrated efficacy in early clinical trials (Friedberg et al., 2010; Hendriks, 2011; Herman et al., 2011; Lannutti et al., 2011; Robertson et al., 2007), subtype-specific effector pathways and underlying genetic mechanisms are incompletely understood. In addition, the consequences of inhibiting BCR signaling in tumors assigned to different transcriptional subtypes require further definition. Herein, we characterize the downstream signaling, apoptotic, and metabolic pathways altered by chemical or molecular SYK inhibition and identify additional genetic bases for enhanced BCR signaling in DLBCLs.

RESULTS

SYK Depletion Selectively Inhibits the Proliferation of BCR-Dependent DLBCL Cell Lines

To further characterize SYK as a potential target, we depleted SYK with multiple independent shRNAs, then assessed cellular proliferation in a panel of DLBCL cell lines that captured known functional distinctions: BCR dependence versus independence and ABC versus GC transcriptional subtype. The panel included BCR-dependent/GC lines (DHL4 and LY7), BCR-dependent/ABC lines (HBL-1 and U-2932), and BCR-independent lines (K422 and LY4, otherwise classified as "OxPhos") (Caro et al., 2012; Chen et al., 2008; Figures S1A–S1E available online). SYK knockdown significantly decreased the proliferation of all BCR-dependent lines but had little effect on the growth of BCR-independent lines (Figures 1A and 1B; Figure S1F). The selectivity of molecular SYK depletion for BCR-dependent DLBCLs closely mirrors that of the chemical SYK inhibitor, R406 (Figure 1B; Figures S1D–S1F; Chen et al., 2008).

SYK- and PI3K-Dependent BCR Signaling in DLBCLs with High Baseline NF-κB

A subset of DLBCL primary tumors and cell lines exhibits high baseline NF-κB activity and multiple genetic alterations of NF-κB pathway components (Compagno et al., 2009; Davis et al., 2001; Lenz et al., 2008). We therefore characterized signaling pathways affected by SYK inhibition in DLBCLs with high versus low baseline NF-κB activity. First, we assessed the baseline NF-κB activity in a panel of eight DLBCL cell lines,

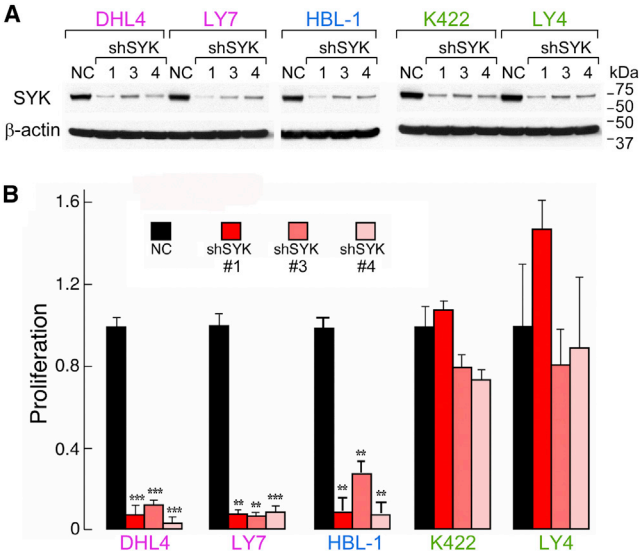

Figure 1. Cellular Proliferation of DLBCL Cell Lines following SYK Depletion

(A) The SYK protein level in cell lysates prepared from the indicated cell lines transduced with a negative control (NC) shRNA or the indicated SYK shRNAs was assessed by immunoblotting. β-actin, loading control.

(B) Cellular proliferation of SYK-depleted DLBCL cell lines was measured 72 hr after puromycin selection by MTS assay. The proliferation of SYK-depleted cells is relative to that of NC cells. Error bars represent SD of three independent assays from a representative experiment. The p values for NC versus each SYK shRNA were determined with a one-sided Welch t test. ***$p \leq 0.0001$; **$p \leq 0.001$.

See also Figure S1.

including the six used above and an additional BCR-dependent/GC line (DHL6) and another BCR-independent (Toledo) line (Chen et al., 2008; Caro et al., 2012). As expected, baseline NF-κB activity was higher in the BCR-dependent/ABC lines than in the BCR-dependent/GC lines (Figure 2A; Davis et al., 2001). R406 treatment significantly decreased the high baseline NF-κB activity in HBL-1 and U-2932 and also reduced the low baseline activity in DHL4, DHL6, and LY7, but had no effect on the BCR-independent lines (Figure 2A).

To further characterize the consequences of chemical SYK inhibition in the BCR-dependent DLBCL cell lines with high or low baseline NF-κB activity, we performed transcriptional profiling of all five lines at baseline and following 6 and 24 hr treatment with R406 or DMSO (vehicle). At each time point, the genes that were differentially expressed between the vehicle and R406-treated samples (FDR-corrected q-values ≤ 0.01 and fold changes $\geq 1.5\times$) were analyzed for pathway enrichment (Figures S2A–S2C; Table S1).

In contrast to the NF-κB-low lines, NF-κB-high lines exhibited significant downregulation of TNF, TNFR2, NF-κB, CD40, and RELA pathway components including multiple common NF-κB target genes (Figures S2B and S2C; Table S1). Independently, we also performed gene set enrichment analysis (GSEA) of vehicle- versus R406-treated cell lines using functionally defined series of NF-κB target genes (Davis et al., 2010; Schreiber et al., 2006). With this approach, we identified statistically significant, concordant downregulation of multiple functionally validated NF-κB target genes in the NF-κB-high DLBCL cell lines following R406 treatment (Figures 2B and 2C). In contrast, GSEA revealed no significant modulation of NF-κB target gene sets in the NF-κB-low DLBCL cell lines (data not shown). We further assessed the transcript abundance of 4 of these NF-κB targets (BCL2A1 [also known as BFL-1/A1], TNF, CD40, and TRAF1; Figure 2C) in the full series of eight DLBCL lines treated with vehicle or R406 using qRT-PCR. All four NF-κB targets were selectively and significantly downregulated in the BCR-dependent NF-κB-high DLBCL cell lines (Figure 2D; Figure S2D).

Given the demonstrated role of the NF-κB target, BCL2A1, in B cell survival and resistance to apoptosis (Lee et al., 1999; Ottina et al., 2012; Zong et al., 1999), we also evaluated BCL2A1 protein expression in DLBCLs treated with vehicle or R406. The two BCR-dependent NF-κB-high lines, HBL-1 and U-2932, had abundant baseline BCL2A1 protein expression that decreased following R406 treatment whereas BCR-dependent NF-κB-low lines (DHL4, DHL6, and LY7) and BCR-independent lines (K422, Toledo, and LY4) had much lower BCL2A1 expression (Figure 2E). We also depleted SYK with multiple independent shRNAs and evaluated BCL2A1 transcript abundance in two BCR-dependent NF-κB-high DLBCL lines (HBL-1 and U-2932) and a BCR-dependent NF-κB-low line (DHL4). SYK knockdown significantly decreased BCL2A1 transcript abundance in the NF-κB-high lines and also reduced the modest BCL2A1 expression in the NF-κB-low line (Figure 2F).

Given the recently described role of PI3K signaling in modulating NF-κB activity in certain DLBCL cell lines (Kloo et al., 2011), we next treated BCR-dependent lines with PI3K inhibitor, LY294002, and evaluated NF-κB activity and BCL2A1 expression. In DLBCL cell lines with high baseline NF-κB (HBL-1 and U-2932), PI3K inhibition significantly decreased NF-κB activity and BCL2A1 abundance (Figures 2G and 2H). Together, these data confirm that NF-κB activity is modulated by BCR-dependent SYK and PI3K signaling in certain "ABC" DLBCL cell lines.

SYK- and PI3K-Dependent BCR Signaling in DLBCLs with Low Baseline NF-κB

Previous murine models of tonic BCR signaling implicated PI3K/AKT activation and FOXO1 modulation in normal B cell survival, independent of NF-κB (Srinivasan et al., 2009). These data prompted us to evaluate the role of PI3K/AKT in BCR-dependent DLBCLs with low baseline NF-κB activity.

Representative BCR-dependent DLBCL cell lines with low baseline NF-κB activity, DHL4, DHL6 and LY7, were infected with either a pMIG empty vector or the pMIG-mAKT1-IRES-GFP (mAKT) vector which encodes constitutively active AKT1. GFP^+ cells were sorted by flow cytometry, treated with R406 or vehicle control and analyzed for p-AKT expression and cellular proliferation. All three BCR-dependent DLBCL cell lines infected with the control pMIG vector exhibited baseline AKT phosphorylation that was inhibited by R406 (Figure 3A). As expected, expression of mAKT increased the level of p-AKT, which was not significantly affected by R406 (Figure 3A). Expression of mAKT largely protected these BCR-dependent DLBCLs from chemical SYK inhibition (Figure 3B). Although mAKT may signal to a larger series of targets than endogenous AKT, these studies nonetheless highlight the role of PI3K/AKT in SYK-dependent survival signals.

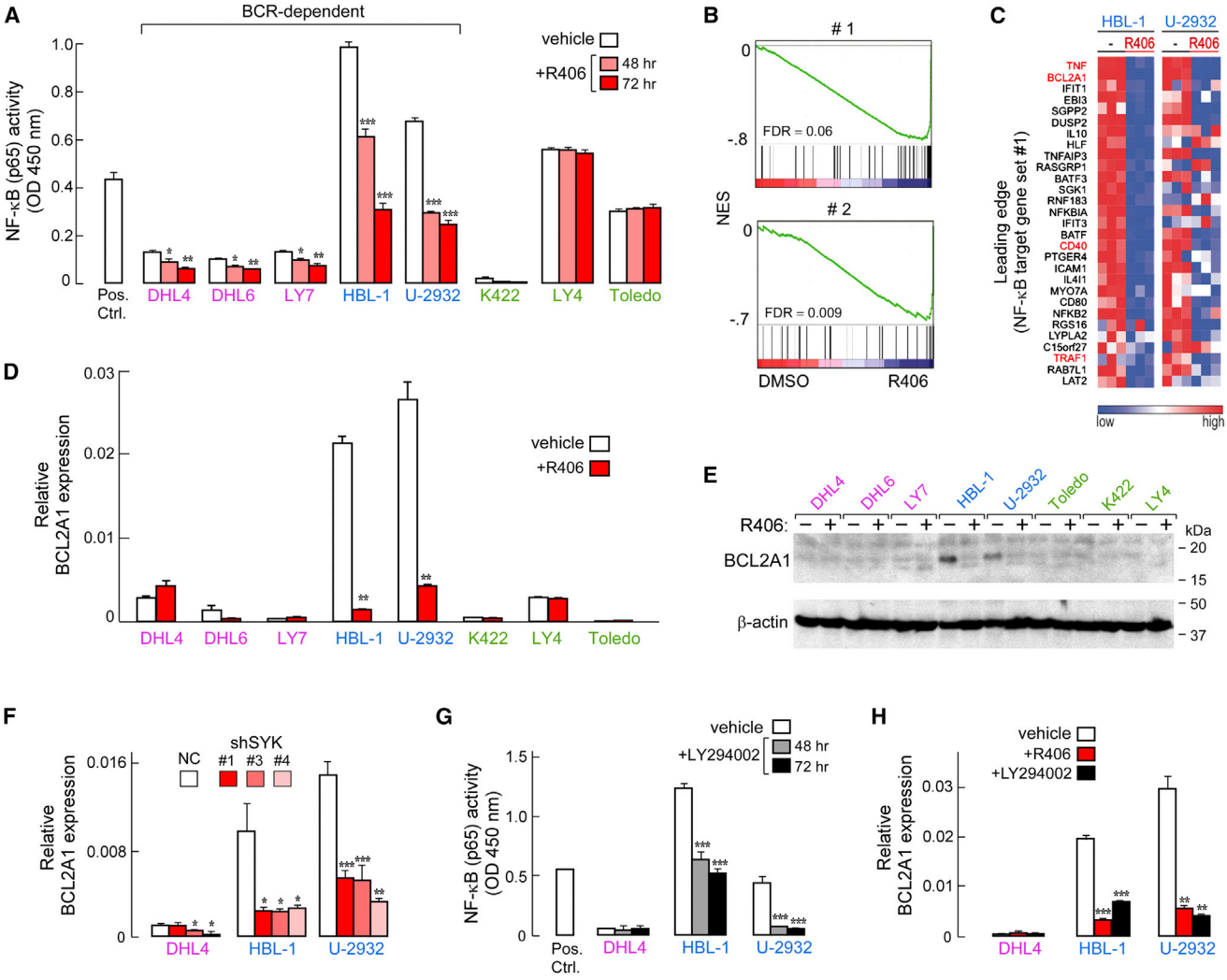

Figure 2. SYK- and PI3K-Dependent BCR Signaling in DLBCLs with High Baseline NF-κB

(A) NF-κB (p65) activity was determined in vehicle and R406-treated DLBCL cell lines. Pos. Ctrl., manufacturer's positive control. BCR-dependent NF-κB-low lines, purple; BCR-dependent NF-κB-high lines, blue; BCR-independent OxPhos lines, green.

(B) GSEA of NF-κB targets was performed in vehicle- versus R406-treated DLBCL cell lines with high-baseline NF-κB activity (HBL-1 and U-2932). The 19K genes in the genome were sorted from highest (left, red) to lowest (right, blue) relative expression in vehicle- versus R406-treated lines (horizontal axis). Note that the positions of the NF-κB targets (set #1, Davis et al., 2010; and set #2, Schreiber et al., 2006) were significantly skewed toward the right end of the sorted list, reflecting their statistically significant downregulation in R406-treated lines.

(C) Relative abundance of NF-κB target genes in vehicle- versus R406-treated DLBCL cell lines with high baseline NF-κB activity was displayed with a colometric scale. NF-κB target genes derived from the GSEA leading edge, set #1 (Davis et al., 2010).

(D) BCL2A1 transcript abundance in DLBCL cell lines treated with vehicle or R406 (24 hr) was determined by qRT-PCR relative to PPIA.

(E) BCL2A1 protein abundance in vehicle- and R406-treated DLBCL cell lines was assessed by immunoblotting. β-actin, loading control.

(F) BCL2A1 transcript abundance in SYK-depleted DLBCL cell lines (72 hr following completion of puromycin selection) was determined by qRT-PCR relative to PPIA.

(G) NF-κB (p65) activity was determined in DLBCL cell lines treated with the PI3K inhibitor LY294002 or vehicle.

(H) BCL2A1 transcript abundance in DLBCL cell lines treated with LY294002, R406, or vehicle (24 hr) was assessed by qRT-PCR relative to PPIA.

In (A), (D), and (F)–(H), p values for control versus treated were determined with a one-sided Welch t test. ***$p < 0.0001$; **$p < 0.001$; *$p < 0.01$. Error bars represent the SD of three independent assays in a representative experiment.

See also Figure S2 and Table S1.

PI3K/AKT signaling phosphorylates the FOXO1 transcription factor resulting in its nuclear exclusion and degradation and decreased FOXO1 activity (Fu and Tindall, 2008; Srinivasan et al., 2009). Given the role of PI3K/AKT in mediating SYK/BCR survival signals, we assessed nuclear FOXO1 expression in R406-treated BCR-dependent DLBCLs. In addition to directly visualizing FOXO1 by immunofluorescence (Figure 3C, left), nuclear FOXO1 staining was quantified (Figure 3C, right). In each of the BCR-dependent DLBCL cell lines, chemical SYK/BCR inhibition significantly increased the nuclear localization of

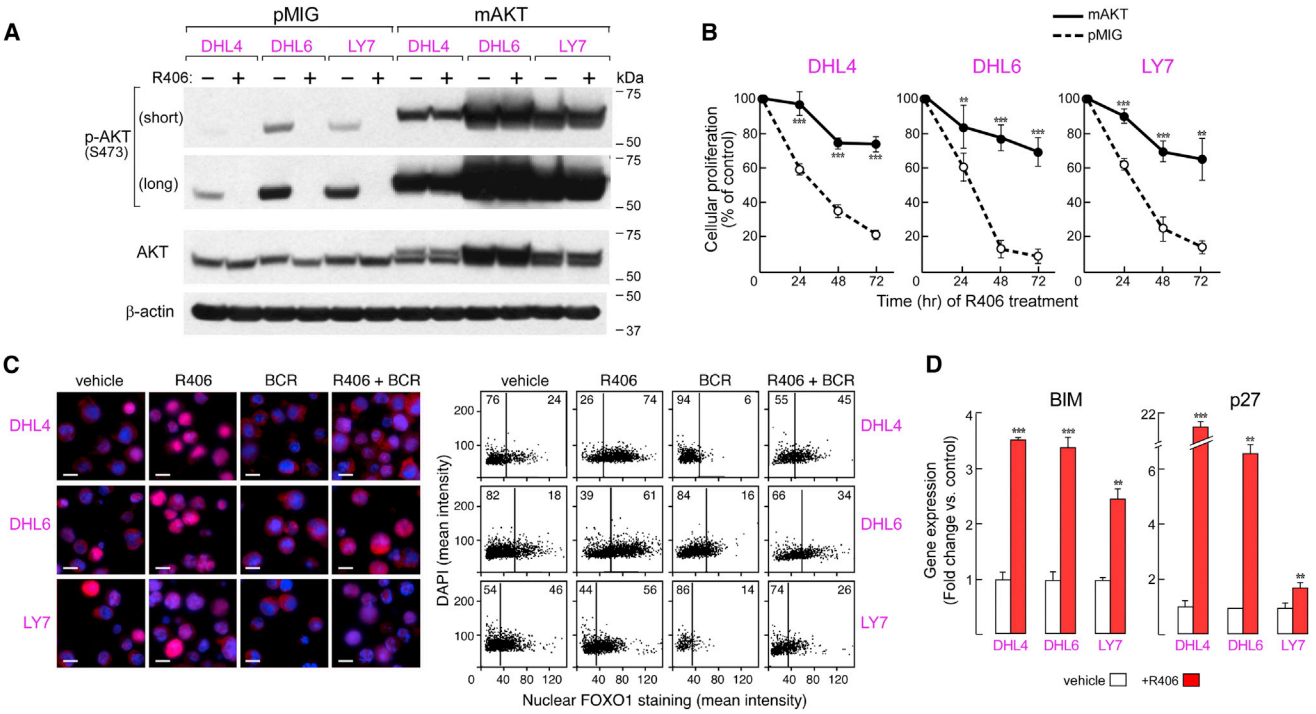

Figure 3. SYK and PI3K-Dependent Signaling in DLBCLs with Low Baseline NF-κB

(A and B) DHL4, DHL6, and LY7 cell lines were retrovirally transduced with mAKT or pMIG vector, FACS-sorted for GFP expression, treated for 24 hr with R406 or vehicle, then analyzed for p-AKT(S473) and total AKT by immunoblotting (A) and for proliferation (B).

(C) DLBCL cell lines were incubated with R406 or vehicle for 1 hr, BCR cross-linked (BCR) or left untreated, fixed, then stained with DAPI (blue) and with Cy3-conjugated anti-FOXO1 antibody (red) (left). Scale bar represents 10 μm. The mean nuclear staining intensity of Cy3-conjugated-FOXO1 was quantified for each cell and plotted against its mean DAPI staining intensity (right).

(D) The transcript abundance of FOXO1 target genes, p27 and BIM, in DLBCL cell lines treated with R406 or vehicle for 24 hr was assessed by qRT-PCR relative to PPIA. The p values for mAKT versus pMIG (control) at each time point (B) and for vehicle versus R406 (D) were determined with a one-sided Welch t test. ***$p \leq 0.0001$; **$p \leq 0.001$. Error bars represent the SD of three independent assays in a representative experiment.

See also Figure S3.

FOXO1 at baseline and following BCR crosslinking (Figure 3C). Similar results were obtained in additional BCR-dependent, but not BCR-independent, DLBCL cell lines (Figures S3A and S3B). Consistent with these observations, R406 treatment selectively induced expression of the FOXO1 target genes, BIM and p27, in BCR-dependent, but not BCR-independent, DLBCL cell lines (Figure 3D; Figure S3C).

SYK Inhibition Induces the Pro-Apoptotic BCL2 Family Member, HRK

We next assessed the transcriptional profiles of R406-treated BCR-dependent NF-κB-low DLBCLs for potential selective apoptotic mechanisms. Differential analysis revealed selective upregulation of the pro-apoptotic BCL2 family member, HRK, in NF-κB-low DLBCLs following chemical SYK inhibition (Figure S4A). Although little is known about the role of HRK in lymphoid cells, this BH3-only protein is specifically induced by growth factor withdrawal in hematopoietic progenitors, leading to cell death (Nakamura et al., 2008; Sanz et al., 2000). For this reason, HRK induction was also evaluated by qRT-PCR in the full panel of BCR-dependent and -independent DLBCL cell lines treated with R406. Chemical SYK inhibition selectively induced HRK in BCR-dependent NF-κB-low cell lines (DHL4, DHL6, and LY7); in contrast, HRK was not comparably upregulated in BCR-dependent NF-κB-high cell lines (HBL-1 and U-2932) or BCR-independent cell lines (K422, LY4, Toledo) (Figure 4A). SYK depletion also selectively induced HRK expression in BCR-dependent DLBCL cell lines with low baseline NF-κB activity (Figure 4B).

Given the role of PI3K/AKT in mediating SYK/BCR survival signals in these DLBCLs (Figure 3B), we asked whether PI3K/AKT also modulated HRK expression. In the BCR-dependent NF-κB-low DLBCL lines, DHL4, DHL6, and LY7, chemical PI3K inhibition (LY294002) was as effective as R406 treatment in inducing HRK (Figure 4C). In each of these lines, expression of mAKT abrogated HRK induction by R406 (Figure 4D). Therefore, BCR signaling actively represses HRK expression via a SYK- and PI3K/AKT-mediated mechanism in BCR-dependent DLBCLs with low baseline NF-κB.

We next assessed the role of HRK in the apoptosis of BCR-dependent NF-κB-low DLBCLs using stable HRK knockdown clones. In these HRK-depleted cells, R406 still inhibited proximal components of the BCR signaling cascade (Figure S4B), but failed to induce HRK (Figure 4E; Figure S4C). Most importantly, R406 did not trigger the apoptosis of HRK-depleted DLBCLs (Figure 4F; Figure S4D). These data directly implicate this

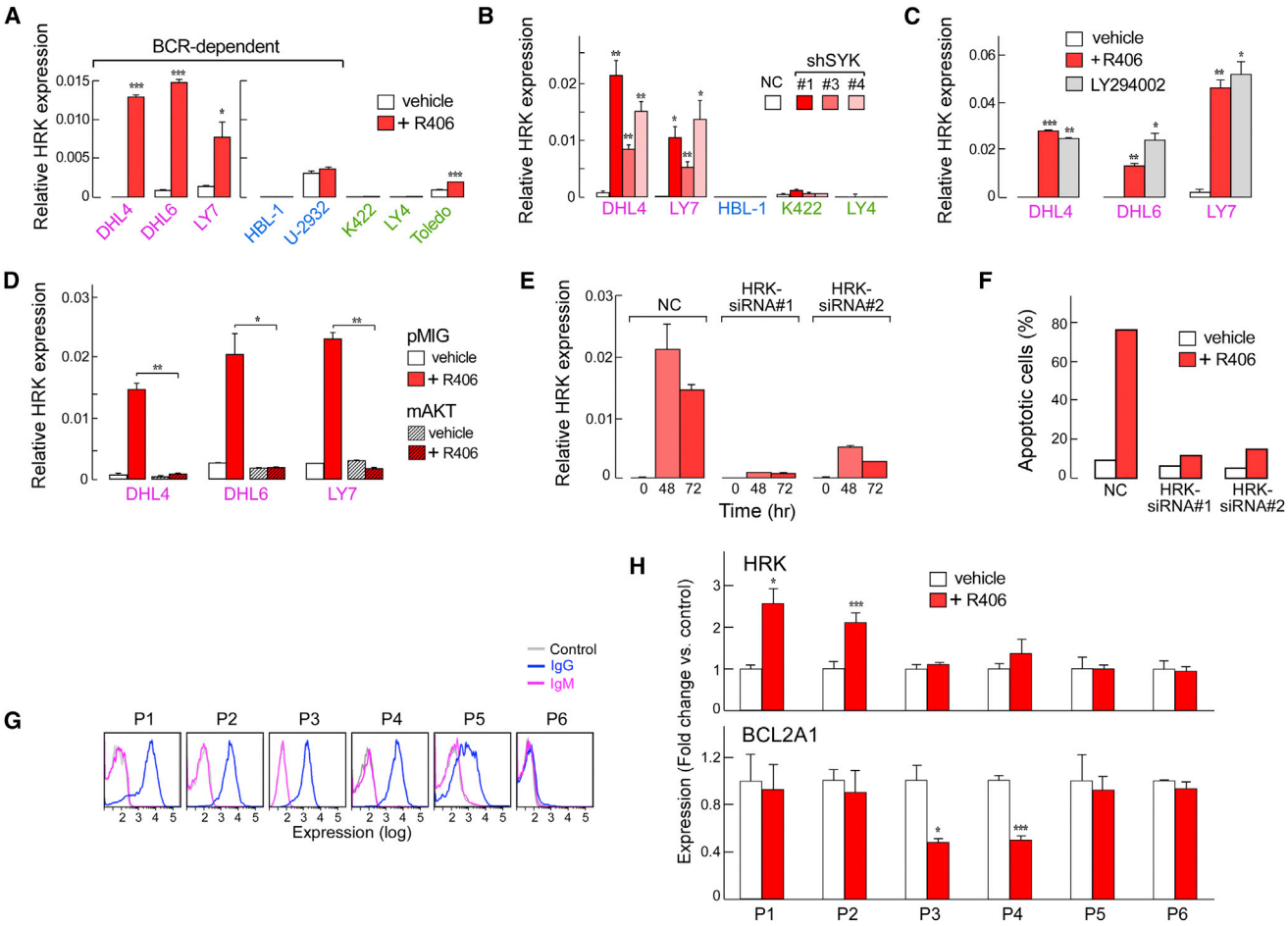

Figure 4. HRK Induction in DLBCL Cell Lines following SYK or PI3K Inhibition

(A) HRK transcript abundance in DLBCL cell lines following R406 treatment (24 hr) was determined by qRT-PCR.

(B) HRK expression in SYK-depleted DLBCL cell lines was assessed by qRT-PCR.

(C) HRK expression in the indicated cell lines following treatment with R406, LY294002, or vehicle for 24 hr assessed by qRT-PCR.

(D) HRK transcript abundance in DLBCL lines transduced with mAKT or pMIG, FACS-sorted, then treated with R406 or vehicle for 24 hr was analyzed by qRT-PCR.

(E) DHL4 cells stably transduced with the indicated HRK siRNA or negative control siRNA (NC) were treated with R406 or vehicle for 24 hr and analyzed for HRK transcript abundance by qRT-PCR.

(F) Apoptosis of DHL4 cells transduced with HRK siRNA or negative control siRNA (NC) and treated with vehicle or R406 for 72 hr was assessed by Annexin V/PI staining.

(G and H) Viable DLBCL tumor cells isolated from cryopreserved primary patient samples were analyzed for cell surface Ig expression (G) or for HRK and BCL2A1 transcript abundance after treatment with R406 or vehicle for 24 hr by qRT-PCR (H). The p values for vehicle versus R406 (A and H), vehicle versus R406 or LY29004 (C), NC versus shSYK (B), and pMIG +R406 versus mAKT +R406 (D) were determined with a one-sided Welch t test. ***p $\leq$ 0.0001; **p $\leq$ 0.001; *p $\leq$ 0.01. Error bars represent the SD of three independent assays in a representative experiment.

See also Figure S4.

BH3-only protein in R406-induced apoptosis of NF-κB-low DLBCLs and indicate that BCR-dependent survival signals include active HRK repression.

Modulation of Survival Pathways in Primary DLBCLs

After defining distinct viability pathways in BCR-dependent DLBCL cell lines with low or high baseline NF-κB activity, we evaluated the same parameters in primary DLBCLs. Viable primary tumor cell suspensions were prepared and aliquots were evaluated for cell-surface Ig or treated with vehicle or R406 and harvested for qRT-PCR analysis of HRK and BCL2A1 transcripts. We identified primary DLBCLs with high surface Ig (P1–P4) or lower/undetectable surface Ig (P5 and P6) (Figure 4G), as previously described (Chen et al., 2008), and assessed p65 nuclear staining in the associated P1-P4 fixed biopsy specimens. Primary tumors P3 and P4 had significantly higher p65 nuclear staining than P1 and P2, indicating that P3 and P4 had higher baseline NF-κB activity (Figures S4E and S2F). In primary DLBCLs with higher baseline NF-κB activity (P3 and P4), R406 treatment significantly decreased BCL2A1 abundance; in contrast, chemical SYK inhibition significantly increased HRK abundance in DLBCLs with lower baseline p65 NF-κB activity

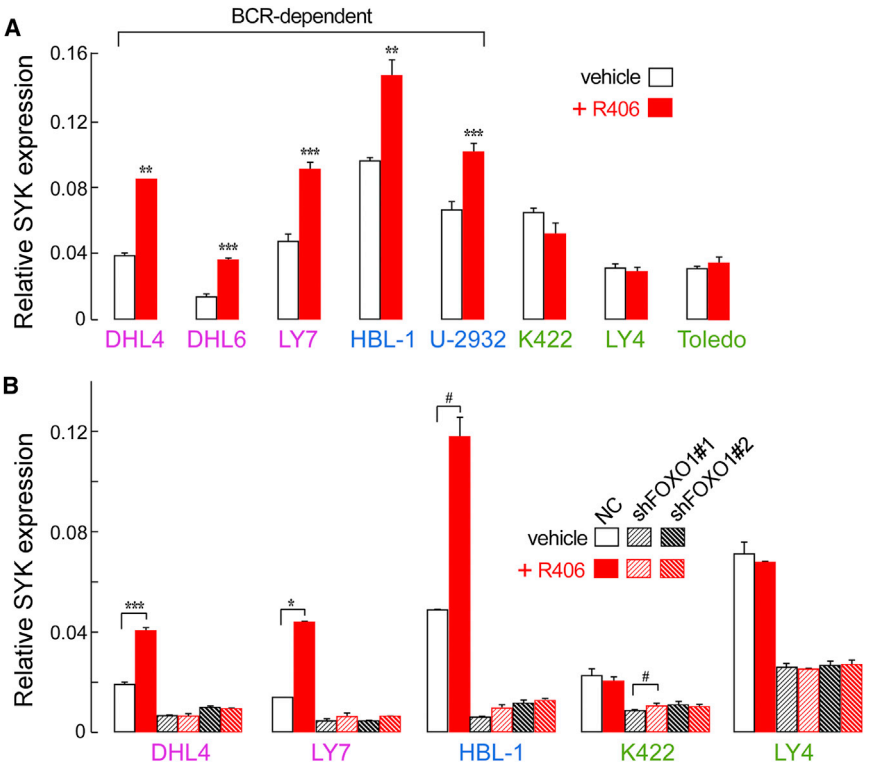

Figure 5. SYK Expression following Chemical SYK Inhibition and FOXO1 Depletion

(A) SYK transcript abundance in DLBCL cell lines was assessed by qRT-PCR following 24 hr of treatment with R406 or vehicle.

(B) SYK transcript abundance in DLBCL cell lines treated with R406 or vehicle for 24 hr following transduction with indicated shRNA was analyzed by qRT-PCR. The p values for vehicle versus R406 were determined with a one-sided Welch t test. ***$p \leq 0.0001$; **$p \leq 0.001$; *$p \leq 0.01$, #, $p \leq 0.05$. Error bars represent the SD of three independent assays in a representative experiment.

See also Figure S5.

(P1 and P2) (Figure 4H). R406 treatment did not alter HRK or BCL2A1 levels in primary DLBCLs with low or no surface Ig (P5 and P6; Figure 4H). Similar results were obtained in additional viable primary tumor cell suspensions (Figures S4G and S4H). Therefore, the distinct survival pathways defined in representative BCR-dependent DLBCL cell lines—SYK- and PI3K-modulated NF-κB signaling or HRK repression—were also operative in primary tumors.

Chemical SYK Inhibition Induces the FOXO1-Dependent Transcriptional Upregulation of SYK

After characterizing distinct viability pathways in BCR-dependent DLBCLs with low- or high-baseline NF-κB, we evaluated the transcription profiles of all five R406-treated BCR-dependent cell lines for potential common features. Pathway analyses revealed transcriptional upregulation of proximal BCR signaling pathway components including CD79B and SYK itself following chemical SYK inhibition (Table S1; Figure S5A). We confirmed the selective upregulation of SYK transcripts and protein in BCR-dependent DLBCLs using the full panel of R406-treated cell lines, qRT-PCR, and intracellular flow cytometry (Figure 5A; Figure S5B). Although R406 treatment increased SYK transcript and total protein abundance, phosphorylation of the downstream BCR signaling component BLNK was inhibited (Figure 5A; Figure S5B). The data suggest that the transcriptional upregulation of certain proximal BCR signaling components may be an attempted, but ineffective, compensatory response to chemical SYK inhibition.

Chemical SYK inhibition increases the nuclear localization of FOXO1 and FOXO1 activity (Figures 3C and 3D; Figures S3A–S3C) and SYK is a recently described FOXO1 target (Ochiai et al., 2012). For these reasons, we assessed the role of FOXO1 in SYK expression. FOXO1 was depleted with two independent shRNAs (Figure S5C) and SYK transcript abundance was assessed by qRT-PCR following vehicle or R406 treatment. In the BCR-dependent DLBCL lines (DHL4, LY7, and HBL-1), the R406-associated induction of SYK was abrogated by FOXO1 knockdown (Figure 5B). Therefore, in BCR-dependent DLBCLs, the attempted compensatory response to chemical SYK inhibition includes FOXO1-mediated transcriptional upregulation of SYK.

SYK/BCR Inhibition Decreases the Abundance of Cholesterol Biosynthesis Pathway Components

Pathway analyses of the five profiled BCR-dependent DLBCL cell lines suggested that chemical SYK inhibition also had important metabolic consequences. R406 treatment downregulated multiple components of the cholesterol biosynthesis pathway, including HMGCS1 (Figure 6A; Table S1; Reed et al., 2008). In the full DLBCL cell line panel, chemical SYK inhibition selectively decreased HMGCS1 protein abundance in BCR-dependent DLBCLs but had no effect on BCR-independent tumors (Figure 6B). SYK depletion similarly decreased HMGCS1 expression in representative BCR-dependent DLBCL cell lines with low or high baseline NF-κB (Figure 6C).

Because cholesterol biosynthesis can be regulated by growth factor- and hormone-induced PI3K/AKT signaling (Krycer et al., 2010; Liu et al., 2009), we assessed the role of PI3K/AKT in R406-mediated downregulation of HMGCS1. In a representative BCR-dependent DLBCL cell line (DHL4), R406 and LY294002 treatment similarly decreased HMGCS1 expression (Figure 6D). In addition, expression of mAKT completely abrogated R406-mediated downregulation of HMGCS1 (Figure 6E). Together, these data indicate that SYK/BCR inhibition modulates sterol biosynthesis via PI3K/AKT.

Each of the SYK/BCR-responsive cholesterol pathway components (Figure 6A) is a known target of SREBP, a PI3K/AKT-dependent transcription factor and master regulator of cholesterol biosynthesis (Krycer et al., 2010; Reed et al., 2008). PI3K/AKT regulation of SREBP occurs at multiple levels, including

FOXO1-mediated repression of SREBP transcripts (Liu et al., 2009; Zhang et al., 2006) and mTORC1 and S6K1-dependent processing of SREBP1 to its active nuclear form (Düvel et al., 2010). In BCR-dependent DLBCLs, R406 treatment also decreased the processing of SREBP1 (Figure S6A).

SYK Blockade Decreases Membrane Cholesterol Content and Inhibits BCR Capping

To assess the functional consequences of SYK/PI3K-dependent cholesterol biosynthesis in DLBCLs, we treated the full panel of DLBCL cell lines with R406 and evaluated cholesterol membrane content. Following R406 or vehicle treatment, DLBCL cell lines were stained with filipin, which forms a fluorescent complex with cholesterol (Gimpl and Gehrig-Burger, 2007; Karnell et al., 2005). Then, filipin flow cytometry was used to quantify and visualize the cellular distribution of cholesterol. SYK/BCR inhibition clearly decreased cholesterol membrane content in BCR-dependent DLBCLs but had no effect on BCR-independent DLBCLs (Figure 6F).

To determine the functional consequences of decreased cholesterol membrane content, we characterized ligand (anti-IgG)-induced BCR redistribution in filipin-stained DLBCLs (Karnell et al., 2005). In BCR-dependent NF-κB-low DLBCLs, filipin-stained cholesterol-enriched membrane domains colocalized with the BCR following anti-Ig induced capping (Figure 6G, +BCR). In contrast, BCR capping and the colocalization of BCR and filipin/cholesterol were markedly decreased following R406 treatment (Figure 6G, +R406/+BCR). Similar results were obtained in two high-NF-κB cell lines, HBL-1 and U-2932 (Figure S6B). These studies indicate that in BCR-dependent DLBCLs, chemical SYK inhibition perturbs the integrity of cholesterol-rich lipid rafts and the association of BCR clusters with these regions.

Genetic Bases for Enhanced BCR Signaling in BCR-Dependent DLBCLs

After defining a role for SYK and PI3K/AKT in the survival of BCR-dependent DLBCL cell lines and primary tumors, we assessed potential genetic bases for the enhanced BCR signaling. Using a well-annotated series of primary DLBCLs with available transcription profiles and high-resolution copy number data (Monti et al., 2012), we evaluated proximal BCR signaling components including SYK and the negative regulator of PI3K/AKT signaling, PTEN. In this primary DLBCL series, there were recurrent single copy gains of *SYK* and monoallelic chromosome 10q23/*PTEN* deletions with associated highly significant changes in transcript abundance (Figure 7A; Figures S7A and S7B; Table S2). These genetic alterations were largely mutually exclusive and significantly more abundant in primary DLBCLs defined as "BCR-type" by transcriptional profiling (Figure 7B; Figures S7A and S7B). Consistent with these findings, PTEN depletion protected one of the three BCR-dependent DLBCL cell lines from chemical SYK inhibition (Figures S7C and S7D).

DISCUSSION

In this study, we characterize distinct SYK/PI3K/AKT-dependent BCR viability pathways in DLBCL cell lines and primary tumors with high- and low-baseline NF-κB activity and define SYK/PI3K/AKT-dependent repression of the pro-apoptotic HRK protein as an important survival mechanism in BCR-dependent NF-κB low DLBCLs (Figure 8A). In addition, we identify SYK/PI3K/AKT-dependent cholesterol biosynthesis as a feed-forward mechanism of preserving the integrity of BCRs in lipid rafts in DLBCLs with low- or high-baseline NF-κB (Figure 8B). Consistent with the roles of SYK and PI3K/AKT as important mediators of BCR survival signals in primary DLBCLs, we also identify *SYK* amplification and *PTEN* deletion as selective and largely mutually exclusive genetic alterations in "BCR"-type tumors.

Our studies highlight the important role of PI3/AKT in the BCR-dependent survival of DLBCLs with high- or low-baseline NF-κB activity. In DLBCLs with high-baseline NF-κB activity, genetic alterations of multiple NF-κB pathway components have been described (Compagno et al., 2009; Lenz et al., 2008; Ngo et al., 2011) and additional *CD79A* and *CD79B* mutations have been reported (Davis et al., 2010). However, the sensitivity of DLBCLs with high baseline NF-κB activity to inhibition of upstream BCR signals was incompletely defined. In this study, chemical SYK blockade and molecular SYK depletion decreased NF-κB activity and target gene expression in DLBCL primary tumors and cell lines with high-baseline NF-κB, including lines with wild-type *CARD11* and either wild-type *CD79B* (U-2932) or *CD79B* missense mutations (HBL-1) (Davis et al., 2010). Chemical PI3K inhibition had similar effects. Taken together, these studies indicate that DLBCLs with high-baseline NF-κB activity remain sensitive to inhibition of proximal SYK/PI3K signals.

In BCR-dependent DLBCL cell lines and primary tumors with low-baseline NF-κB activity, both the chemical inhibition and molecular depletion of SYK induced the pro-apoptotic HRK protein via a PI3K/AKT-dependent mechanism. HRK depletion abrogated R406-induced cytotoxicity in these cells. These data highlight the previously unappreciated role of this BH3-only protein in DLBCL apoptosis and indicate that BCR-dependent survival signals include active HRK repression. These observations are consistent with earlier studies in which HRK was actively repressed at baseline and specifically induced following growth factor withdrawal in hematopoietic progenitors and neuronal cells (Nakamura et al., 2008; Sanz et al., 2001; Towers et al., 2009). In these experimental settings, HRK induction led to rapid cell death, as in our study. Additional genetic bases of HRK repression, such as hypermethylation and allelic loss, have been described in certain cancers including primary central nervous system lymphomas (Nakamura et al., 2008).

In our studies, molecular SYK depletion phenocopies chemical SYK inhibition in a panel of BCR-dependent and -independent DLBCL cell lines. Similar results were recently described in an overlapping series of DLBCL cell lines (Cheng et al., 2011). In BCR-dependent DLBCLs, R406 treatment induces FOXO1-mediated transcriptional upregulation of SYK, indicating that SYK is a tightly regulated component of the BCR signaling and survival pathway.

Chemical SYK inhibition also selectively decreased multiple components of the cholesterol biosynthesis pathway. SYK/BCR inhibition modulated cholesterol biosynthesis via PI3K/AKT and implicated the PI3K/AKT-dependent transcription factor and master regulator of cholesterol biosynthesis, SREBP

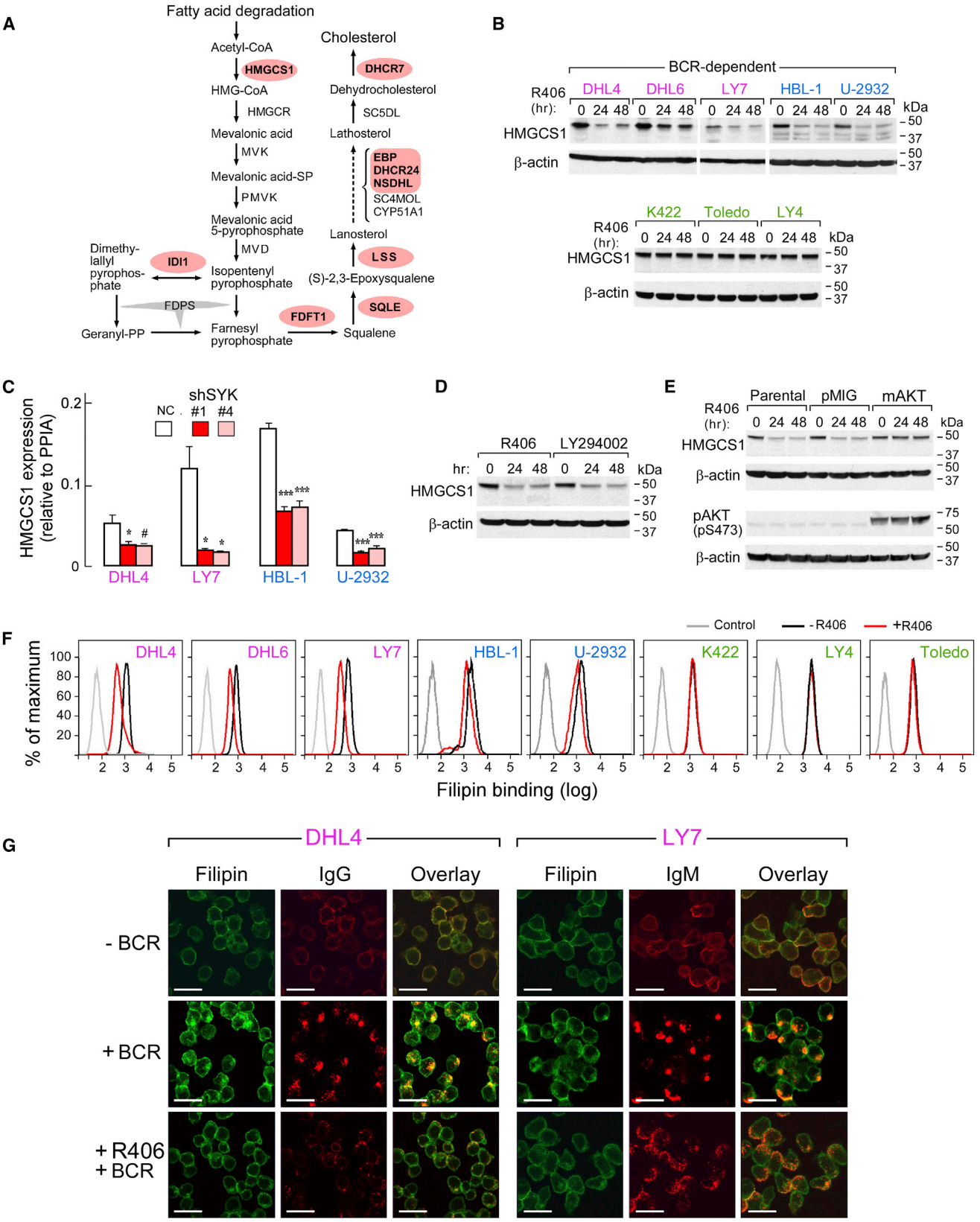

(legend on next page)

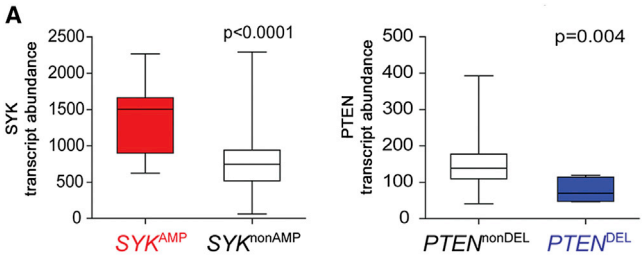

B

	SYK^{AMP} n(%)	SYK^{nonAMP} n(%)
BCR	8 (73)	42 (31)
Other	3 (27)	94 (69)
Total	11 (100)	136 (100)

p=0.008

	$PTEN^{nonDEL}$ n(%)	$PTEN^{DEL}$ n(%)
BCR	45 (32)	5 (83)
Other	96 (68)	1 (17)
Total	141 (100)	6 (100)

p=0.018

Figure 7. *SYK* and *PTEN* Copy Number Alterations in Primary DLBCLs

(A) *SYK* and *PTEN* copy numbers were assessed and associated with SYK and PTEN transcript levels in primary DLBCLs (n = 169). *SYK* and *PTEN* copy numbers and transcript abundance were derived from (Monti et al., 2012). The p values were determined with a one-sided t test. Box plot (median, line; 25% and 75% quartile, box; whiskers, maximum to minimum).

(B) Relative frequency of SYK^{AMP} and $PTEN^{DEL}$ was assessed in transcriptionally defined "BCR" type versus other primary DLBCLs (n = 147; tumors with high confidence classification into CCC categories) (Monti et al., 2012). The p values were determined with a two-sided Fisher exact test.

See also Figure S7 and Table S2.

(Bengoechea-Alonso and Ericsson, 2007; Krycer et al., 2010; Porstmann et al., 2008). In BCR-dependent DLBCLs, R406-treatment also decreased cholesterol membrane content and perturbed the integrity of cholesterol-rich lipid rafts and the association of BCR clusters with these membrane domains (Gupta and DeFranco, 2007). Therefore, in addition to directly modulating downstream apoptotic pathways, chemical SYK inhibition alters cholesterol biosynthesis, with associated adverse consequences for cell membrane integrity and the assembly of BCR clusters.

The modulation of cholesterol biosynthesis by SYK is of additional interest given the recently described distinct metabolic profiles in BCR-dependent and BCR-independent/OxPhos DLBCLs (Caro et al., 2012). In BCR-dependent DLBCLs, SYK signaling limits the mitochondrial oxidation of fatty acids (Caro et al., 2012), which likely ensures the availability of metabolic intermediates such as acetyl CoA for HMGCS1-mediated cholesterol biosynthesis. In comparison, acetyl-CoA derived from fatty acid enters the tricarboxylic acid cycle in BCR-independent/OxPhos DLBCLs that exhibit increased mitochondrial fatty acid oxidation (Caro et al., 2012). These findings further define molecular subsets of DLBCLs with distinct metabolic features that are linked to the functional state of upstream BCR signaling components.

We previously found that BCR-dependent DLBCL cell lines and primary tumors with low baseline NF-κB activity also responded to SYK/BCR inhibition (Chen et al., 2008). However, it was unclear whether these DLBCLs had uncharacterized genetic alterations of BCR signaling pathway components or preserved reliance on physiologic "tonic" BCR survival signals. In the current analysis of an extensive series of newly diagnosed primary DLBCLs, *SYK* amplification and *PTEN* deletion were identified as largely mutually exclusive genetic alterations in transcriptionally-defined "BCR-type" DLBCLs. Given the role of PI3K/AKT in SYK/BCR-dependent survival signals in DLBCLs, these data suggest additional genetic bases for increased BCR pathway activity in these tumors.

Taken together, these functional and genetic studies provide a framework for analyzing targeted inhibition of SYK, PI3K and additional proximal components of the BCR signaling pathway in BCR-dependent DLBCLs and set the stage for further clinical analysis of promising candidate inhibitors.

EXPERIMENTAL PROCEDURES

Cell lines and culture conditions are in Supplemental Experimental Procedures. BCR crosslinking was performed as previously described (Chen et al., 2008).

Primary Tumor Specimens

Cryopreserved viable primary DLBCL samples were obtained according to Institutional Review Board (IRB)-approved protocols from Mayo Clinic, Brigham and Women's Hospital and the Dana-Farber Cancer Institute. These anonymous primary tumor specimens were considered discarded tissues that did not require informed consent.

Chemical Inhibition with R406 or LY294002

For immediate inhibition, cells were incubated with 1 μM R406 or vehicle alone (in PBS) in a 37°C water bath for 1 hr. For long-term inhibition, compounds (R406 [1 μM or 4 μM] or LY29004 [10 μM]) were added to cell culture medium at the final indicated concentration and cells were maintained in a 37°C

Figure 6. Cholesterol Biosynthesis in DLBCLs following SYK or PI3K Inhibition

(A) Components of the cholesterol biosynthesis pathway modulated by R406 treatment (red) were identified by pathway analyses of the profiled cell lines.

(B) HMGCS1 protein abundance in R406- or vehicle-treated DLBCL cell lines was assessed by immunoblotting. β-actin, loading control.

(C) HMGCS1 transcript abundance in DLBCL cell lines transduced with indicated shRNA was assessed by qRT-PCR. The p values for NC versus shSYK were determined with a one-sided Welch t test. ***p ≤ 0.0001; *p ≤ 0.01; #, p ≤ 0.02. Error bars represent the SD of three independent assays in a representative experiment.

(D) HMGCS1 protein abundance in DHL4 following treatment with R406 or LY294002 was assessed by immunoblotting. β-actin, loading control.

(E) HMGCS1 and p-AKT(S473) in parental DHL4 cells and DHL4 cells transduced with mAKT or pMIG and treated with R406 was determined by immunoblotting. β-actin, loading control.

(F) Membrane cholesterol content in DLBCL cell lines treated with vehicle (black) or R406 (red) for 2 days and fixed with 4% paraformaldehyde was assessed by filipin flow cytometry. Unstained controls in gray. (G) DHL4 and LY7 cells were incubated with vehicle or R406 for 48 hr and left untreated (−BCR) or stimulated with anti-Ig for 10 min (+BCR). The cells were fixed, stained with filipin (green) and the indicated Cy3-conjugated anti-Ig (red), and assessed with confocal microscopy. Scale bar represents 25 μm.

See also Figure S6.

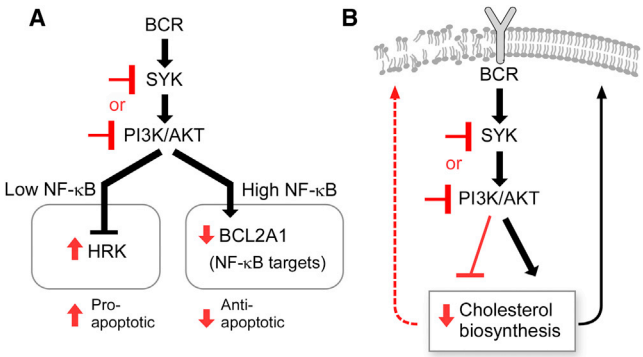

Figure 8. SYK and PI3K-Dependent Viability Pathways in DLBCLs

(A) SYK- and PI3K-dependent anti-apoptotic pathways in BCR-dependent DLBCLs. In BCR-dependent DLBCLs with low-baseline NF-κB activity, SYK or PI3K inhibition relieve BCR-dependent repression of the pro-apoptotic BH3 molecule, HRK. In BCR-dependent DLBCLs with high-baseline NF-κB activity, SYK or PI3K inhibition decreases the abundance of the anti-apoptotic NF-κB targets such as BCL2A1.

(B) SYK- and PI3K-dependent regulation of cholesterol biosynthesis and associated integrity of BCRs in lipid rafts in BCR-dependent DLBCLs.

incubator for 24 or 48 hr. Details are provided in the Supplemental Experimental Procedures.

RNA Interference

Cells were infected with lentivirus containing either negative control (vector pLKO.1-emptyT, TRCN0000208001, Broad Institute, MA) or specific SYK, FOXO1, or PTEN shRNAs, puromycin-selected for 48 hr and analyzed for knockdown efficacy and cellular proliferation thereafter. HRK-specific oligonucleotides or negative control (NC) oligonucleotides were ligated into the linearized pSIREN-RetroQ retroviral vector (Clontech, Mountain View, CA). After retroviral infection and puromycin selection, cells were subcloned by limiting dilution. Selected subclones were treated with R406 or vehicle and efficient HRK knockdown (>75%) was confirmed by qRT-PCR. Details are provided in the Supplemental Experimental Procedures.

Intracellular Flow

Intracellular flow cytometry for p-SYK352, p-BLNK84, total SYK, and PTEN (BD Biosciences, CA) was performed as previously described (Chen et al., 2008).

Immunofluorescence

DLBCL cell lines that were treated with vehicle or R406, with or without subsequent BCR crosslinking, were formalin-fixed, paraffin-embedded, and analyzed for FOXO1 expression and subcellular localization using a rabbit monoclonal anti-FOXO1 antibody (Cell Signaling Technology) and anti-rabbit Cy3-conjugated antibody solution (Invitrogen). The FOXO1-Cy3 stained slides were scanned with a digital FACS imaging system (TissueGnostics, Vienna, Austria) and analyzed with TissueQuest (Tissuegnostics, Vienna, Austria). Details are provided in the Supplemental Experimental Procedures.

Analyses of cellular proliferation and apoptosis, immunoblotting, qRT-PCR, transcriptional profiling and transduction with mAKT are provided in the Supplemental Experimental Procedures.

NF-κB Activity Assay

DLBCL cell lines that were treated with vehicle, R406 or LY294002 were harvested, nuclear extracts were prepared and NF-κB activity was assessed using a TransAM NF-κB family kit and the manufacturer's positive control (Active Motif, Carlsbad, CA). This colorimetric assay detects binding of nuclear (activated) p65 (RELA) to immobilized NF-κB target consensus oligonucleotide sequences as described (Feuerhake et al., 2005).

Filipin Staining

After fixation in 4% paraformaldehyde (1 hr at room temperature) and washes in PBS, cells were incubated in 1 ml PBS-glycine (1.5 mg/ml; 10 min at room temperature) to quench the paraformaldehyde. Thereafter, cells were stained with 1 ml PBS containing 50 μg/ml filipin (1 hr at room temperature) and directly analyzed on a flow cytometer (FACS Canto II, BD Biosciences).

Confocal Microscopy

DLBCL lines (5×10^6 cells) treated with 1 μM R406 or vehicle were harvested and resuspended in 0.5 ml PBS and incubated at 37°C water bath for 20 min. Thereafter, cells were stimulated with Cy3-conjugated AffiniPure $F(ab')_2$ Fragment Goat anti-human IgG or IgM for 10 min, and the reaction was stopped by the addition of cold PBS/0.1% bovine serum albumin/0.02% azide. The cells were fixed in 4% paraformaldehyde/0.1% glutaraldehyde, followed by washing and resuspension in 0.5 mg/ml sodium borohydride to stop fixation. For untreated DLBCL lines that were not BCR crosslinked, cells were fixed with paraformaldehyde before staining with Cy3-conjugated AffiniPure $F(ab')_2$ fragment rabbit anti-goat IgG or IgM. Thereafter, all samples were incubated in PBS containing 50 μg/ml filipin for 1 hr. The cells were adhered to glass slides by centrifugation at 1,200 rpm using cytospin centrifuge (Shandon) and mounted with Prolong Gold anti-fade agent (Invitrogen, Oregon). The cells were visualized using Leica SP5× confocal microscope. Images were captured and analyzed using LAS AF software (Leica Microsystems CMS GmbH).

Analysis of *SYK* and *PTEN* Somatic Copy Number Changes and Transcript Abundance in Primary DLBCLs

SYK and *PTEN* loci copy numbers were assessed and associated with respective SYK and PTEN transcript levels in 169 newly diagnosed DLBCLs (HD-SNP array data and transcriptional profiles from Monti et al., 2012; Gene Expression Omnibus accession number GSE34171). In tumors with SYK^{AMP} versus SYK^{nonAMP} or $PTEN^{DEL}$ versus $PTEN^{nonDEL}$, respective SYK or PTEN transcript levels were visualized with a box plot and evaluated with a Fisher exact test (Dawson-Saunders and Trapp, 1994). The distribution of *SYK* and *PTEN* copy number alterations in BCR versus Other CCC categories was evaluated with a Fisher exact test. Visualization and statistical testing were performed using GraphPad Prism version 5.04 for Windows, GraphPad Software, San Diego, CA, http://www.graphpad.com.

ACCESSION NUMBER

The Gene Expression Omnibus accession number for the gene expression data reported in this paper is GSE43510.

SUPPLEMENTAL INFORMATION

Supplemental Information includes Supplemental Experimental Procedures, seven figures, and two tables and can be found with this article online at http://dx.doi.org/10.1016/j.ccr.2013.05.002.

ACKNOWLEDGMENTS

This work was supported by NIH grants P01CA092625, LLS SCOR 7391, and LLS SCOR 7009.

Received: December 9, 2011
Revised: January 23, 2013
Accepted: May 1, 2013
Published: June 10, 2013

REFERENCES

Bengoechea-Alonso, M.T., and Ericsson, J. (2007). SREBP in signal transduction: cholesterol metabolism and beyond. Curr. Opin. Cell Biol. *19*, 215–222.

Caro, P., Kishan, A.U., Norberg, E., Stanley, I.A., Chapuy, B., Ficarro, S.B., Polak, K., Tondera, D., Gounarides, J., Yin, H., et al. (2012). Metabolic

signatures uncover distinct targets in molecular subsets of diffuse large B cell lymphoma. Cancer Cell *22*, 547–560.

Chen, L., Juszczynski, P., Takeyama, K., Aguiar, R.C., and Shipp, M.A. (2006). Protein tyrosine phosphatase receptor-type O truncated (PTPROt) regulates SYK phosphorylation, proximal B-cell-receptor signaling, and cellular proliferation. Blood *108*, 3428–3433.

Chen, L., Monti, S., Juszczynski, P., Daley, J., Chen, W., Witzig, T.E., Habermann, T.M., Kutok, J.L., and Shipp, M.A. (2008). SYK-dependent tonic B-cell receptor signaling is a rational treatment target in diffuse large B-cell lymphoma. Blood *111*, 2230–2237.

Cheng, S., Coffey, G., Zhang, X.H., Shaknovich, R., Song, Z., Lu, P., Pandey, A., Melnick, A.M., Sinha, U., and Wang, Y.L. (2011). SYK inhibition and response prediction in diffuse large B-cell lymphoma. Blood *118*, 6342–6352.

Compagno, M., Lim, W.K., Grunn, A., Nandula, S.V., Brahmachary, M., Shen, Q., Bertoni, F., Ponzoni, M., Scandurra, M., Califano, A., et al. (2009). Mutations of multiple genes cause deregulation of NF-kappaB in diffuse large B-cell lymphoma. Nature *459*, 717–721.

Davis, R.E., Brown, K.D., Siebenlist, U., and Staudt, L.M. (2001). Constitutive nuclear factor kappaB activity is required for survival of activated B cell-like diffuse large B cell lymphoma cells. J. Exp. Med. *194*, 1861–1874.

Davis, R.E., Ngo, V.N., Lenz, G., Tolar, P., Young, R.M., Romesser, P.B., Kohlhammer, H., Lamy, L., Zhao, H., Yang, Y., et al. (2010). Chronic active B-cell-receptor signalling in diffuse large B-cell lymphoma. Nature *463*, 88–92.

Dawson-Saunders, B., and Trapp, R.G. (1994). Basic and clinical biostatistics (Norwalk, CT: Appleton & Lange).

Düvel, K., Yecies, J.L., Menon, S., Raman, P., Lipovsky, A.I., Souza, A.L., Triantafellow, E., Ma, Q., Gorski, R., Cleaver, S., et al. (2010). Activation of a metabolic gene regulatory network downstream of mTOR complex 1. Mol. Cell *39*, 171–183.

Dykstra, M., Cherukuri, A., Sohn, H.W., Tzeng, S.J., and Pierce, S.K. (2003). Location is everything: lipid rafts and immune cell signaling. Annu. Rev. Immunol. *21*, 457–481.

Feuerhake, F., Kutok, J.L., Monti, S., Chen, W., LaCasce, A.S., Cattoretti, G., Kurtin, P., Pinkus, G.S., de Leval, L., Harris, N.L., et al. (2005). NFkappaB activity, function, and target-gene signatures in primary mediastinal large B-cell lymphoma and diffuse large B-cell lymphoma subtypes. Blood *106*, 1392–1399.

Friedberg, J.W., Sharman, J., Sweetenham, J., Johnston, P.B., Vose, J.M., Lacasce, A., Schaefer-Cutillo, J., De Vos, S., Sinha, R., Leonard, J.P., et al. (2010). Inhibition of Syk with fostamatinib disodium has significant clinical activity in non-Hodgkin lymphoma and chronic lymphocytic leukemia. Blood *115*, 2578–2585.

Fu, Z., and Tindall, D.J. (2008). FOXOs, cancer and regulation of apoptosis. Oncogene *27*, 2312–2319.

Gimpl, G., and Gehrig-Burger, K. (2007). Cholesterol reporter molecules. Biosci. Rep. *27*, 335–358.

Gupta, N., and DeFranco, A.L. (2007). Lipid rafts and B cell signaling. Semin. Cell Dev. Biol. *18*, 616–626.

Hendriks, R.W. (2011). Drug discovery: New Btk inhibitor holds promise. Nat. Chem. Biol. *7*, 4–5.

Herman, S.E., Gordon, A.L., Hertlein, E., Ramanunni, A., Zhang, X.D., Jaglowski, S., Flynn, J., Jones, J., Blum, K.A., Buggy, J.J., et al. (2011). Bruton tyrosine kinase represents a promising therapeutic target for treatment of chronic lymphocytic leukemia and is effectively targeted by PCI-32765. Blood *117*, 6287–6296.

Karnell, F.G., Brezski, R.J., King, L.B., Silverman, M.A., and Monroe, J.G. (2005). Membrane cholesterol content accounts for developmental differences in surface B cell receptor compartmentalization and signaling. J. Biol. Chem. *280*, 25621–25628.

Kloo, B., Nagel, D., Pfeifer, M., Grau, M., Düwel, M., Vincendeau, M., Dörken, B., Lenz, P., Lenz, G., and Krappmann, D. (2011). Critical role of PI3K signaling for NF-kappaB-dependent survival in a subset of activated B-cell-like diffuse large B-cell lymphoma cells. Proc. Natl. Acad. Sci. USA *108*, 272–277.

Kraus, M., Alimzhanov, M.B., Rajewsky, N., and Rajewsky, K. (2004). Survival of resting mature B lymphocytes depends on BCR signaling via the Igalpha/beta heterodimer. Cell *117*, 787–800.

Krycer, J.R., Sharpe, L.J., Luu, W., and Brown, A.J. (2010). The Akt-SREBP nexus: cell signaling meets lipid metabolism. Trends Endocrinol. Metab. *21*, 268–276.

Küppers, R. (2005). Mechanisms of B-cell lymphoma pathogenesis. Nat. Rev. Cancer *5*, 251–262.

Lam, K.P., Kühn, R., and Rajewsky, K. (1997). In vivo ablation of surface immunoglobulin on mature B cells by inducible gene targeting results in rapid cell death. Cell *90*, 1073–1083.

Lannutti, B.J., Meadows, S.A., Herman, S.E., Kashishian, A., Steiner, B., Johnson, A.J., Byrd, J.C., Tyner, J.W., Loriaux, M.M., Deininger, M., et al. (2011). CAL-101, a p110delta selective phosphatidylinositol-3-kinase inhibitor for the treatment of B-cell malignancies, inhibits PI3K signaling and cellular viability. Blood *117*, 591–594.

Lee, H.H., Dadgostar, H., Cheng, Q., Shu, J., and Cheng, G. (1999). NF-kappaB-mediated up-regulation of Bcl-x and Bfl-1/A1 is required for CD40 survival signaling in B lymphocytes. Proc. Natl. Acad. Sci. USA *96*, 9136–9141.

Lenz, G., Davis, R.E., Ngo, V.N., Lam, L., George, T.C., Wright, G.W., Dave, S.S., Zhao, H., Xu, W., Rosenwald, A., et al. (2008). Oncogenic CARD11 mutations in human diffuse large B cell lymphoma. Science *319*, 1676–1679.

Liu, Z., Rudd, M.D., Hernandez-Gonzalez, I., Gonzalez-Robayna, I., Fan, H.-Y., Zeleznik, A.J., and Richards, J.S. (2009). FSH and FOXO1 regulate genes in the sterol/steroid and lipid biosynthetic pathways in granulosa cells. Mol. Endocrinol. *23*, 649–661.

Monroe, J.G. (2006). ITAM-mediated tonic signalling through pre-BCR and BCR complexes. Nat. Rev. Immunol. *6*, 283–294.

Monti, S., Savage, K.J., Kutok, J.L., Feuerhake, F., Kurtin, P., Mihm, M., Wu, B., Pasqualucci, L., Neuberg, D., Aguiar, R.C., et al. (2005). Molecular profiling of diffuse large B-cell lymphoma identifies robust subtypes including one characterized by host inflammatory response. Blood *105*, 1851–1861.

Monti, S., Chapuy, B., Takeyama, K., Rodig, S.J., Hao, Y., Yeda, K.T., Inguilizian, H., Mermel, C., Currie, T., Dogan, A., et al. (2012). Integrative analysis reveals an outcome-associated and targetable pattern of p53 and cell cycle deregulation in diffuse large B cell lymphoma. Cancer Cell *22*, 359–372.

Nakamura, M., Shimada, K., and Konishi, N. (2008). The role of HRK gene in human cancer. Oncogene *27*(*Suppl 1*), S105–S113.

Ngo, V.N., Young, R.M., Schmitz, R., Jhavar, S., Xiao, W., Lim, K.H., Kohlhammer, H., Xu, W., Yang, Y., Zhao, H., et al. (2011). Oncogenically active MYD88 mutations in human lymphoma. Nature *470*, 115–119.

Ochiai, K., Maienschein-Cline, M., Mandal, M., Triggs, J.R., Bertolino, E., Sciammas, R., Dinner, A.R., Clark, M.R., and Singh, H. (2012). A self-reinforcing regulatory network triggered by limiting IL-7 activates pre-BCR signaling and differentiation. Nat. Immunol. *13*, 300–307.

Ottina, E., Grespi, F., Tischner, D., Soratroi, C., Geley, S., Ploner, A., Reichardt, H.M., Villunger, A., and Herold, M.J. (2012). Targeting antiapoptotic A1/Bfl-1 by in vivo RNAi reveals multiple roles in leukocyte development in mice. Blood *119*, 6032–6042.

Porstmann, T., Santos, C.R., Griffiths, B., Cully, M., Wu, M., Leevers, S., Griffiths, J.R., Chung, Y.-L., and Schulze, A. (2008). SREBP activity is regulated by mTORC1 and contributes to Akt-dependent cell growth. Cell Metab. *8*, 224–236.

Reed, B.D., Charos, A.E., Szekely, A.M., Weissman, S.M., and Snyder, M. (2008). Genome-wide occupancy of SREBP1 and its partners NFY and SP1 reveals novel functional roles and combinatorial regulation of distinct classes of genes. PLoS Genet. *4*, e1000133.

Rinaldi, A., Ponzoni, M., Uccella, S., Rossi, D., Gaidano, G., Facchetti, F., Pruneri, G., Tibiletti, M.G., Capella, C., Zucca, E., et al. (2011). In vitro efficacy of tyrosine kinase inhibitors: SYK and BCR-ABL inhibitors in lymphomas. Hematol. Oncol. *29*, 164–166.

Robertson, M.J., Kahl, B.S., Vose, J.M., de Vos, S., Laughlin, M., Flynn, P.J., Rowland, K., Cruz, J.C., Goldberg, S.L., Musib, L., et al. (2007). Phase II study

of enzastaurin, a protein kinase C beta inhibitor, in patients with relapsed or refractory diffuse large B-cell lymphoma. J. Clin. Oncol. *25*, 1741–1746.

Rosenwald, A., Wright, G., Chan, W.C., Connors, J.M., Campo, E., Fisher, R.I., Gascoyne, R.D., Muller-Hermelink, H.K., Smeland, E.B., Giltnane, J.M., et al.; Lymphoma/Leukemia Molecular Profiling Project. (2002). The use of molecular profiling to predict survival after chemotherapy for diffuse large-B-cell lymphoma. N. Engl. J. Med. *346*, 1937–1947.

Sanz, C., Benito, A., Inohara, N., Ekhterae, D., Nunez, G., and Fernandez-Luna, J.L. (2000). Specific and rapid induction of the proapoptotic protein Hrk after growth factor withdrawal in hematopoietic progenitor cells. Blood *95*, 2742–2747.

Sanz, C., Mellstrom, B., Link, W.A., Naranjo, J.R., and Fernandez-Luna, J.L. (2001). Interleukin 3-dependent activation of DREAM is involved in transcriptional silencing of the apoptotic Hrk gene in hematopoietic progenitor cells. EMBO J. *20*, 2286–2292.

Schreiber, J., Jenner, R.G., Murray, H.L., Gerber, G.K., Gifford, D.K., and Young, R.A. (2006). Coordinated binding of NF-kappaB family members in the response of human cells to lipopolysaccharide. Proc. Natl. Acad. Sci. USA *103*, 5899–5904.

Srinivasan, L., Sasaki, Y., Calado, D.P., Zhang, B., Paik, J.H., DePinho, R.A., Kutok, J.L., Kearney, J.F., Otipoby, K.L., and Rajewsky, K. (2009). PI3 kinase signals BCR-dependent mature B cell survival. Cell *139*, 573–586.

Torres, R.M., Flaswinkel, H., Reth, M., and Rajewsky, K. (1996). Aberrant B cell development and immune response in mice with a compromised BCR complex. Science *272*, 1804–1808.

Towers, E., Gilley, J., Randall, R., Hughes, R., Kristiansen, M., and Ham, J. (2009). The proapoptotic dp5 gene is a direct target of the MLK-JNK-c-Jun pathway in sympathetic neurons. Nucleic Acids Res. *37*, 3044–3060.

Wright, G., Tan, B., Rosenwald, A., Hurt, E.H., Wiestner, A., and Staudt, L.M. (2003). A gene expression-based method to diagnose clinically distinct subgroups of diffuse large B cell lymphoma. Proc. Natl. Acad. Sci. USA *100*, 9991–9996.

Young, R.M., Hardy, I.R., Clarke, R.L., Lundy, N., Pine, P., Turner, B.C., Potter, T.A., and Refaeli, Y. (2009). Mouse models of non-Hodgkin lymphoma reveal Syk as an important therapeutic target. Blood *113*, 2508–2516.

Zhang, W., Patil, S., Chauhan, B., Guo, S., Powell, D.R., Le, J., Klotsas, A., Matika, R., Xiao, X., Franks, R., et al. (2006). FoxO1 regulates multiple metabolic pathways in the liver: effects on gluconeogenic, glycolytic, and lipogenic gene expression. J. Biol. Chem. *281*, 10105–10117.

Zong, W.X., Edelstein, L.C., Chen, C., Bash, J., and Gélinas, C. (1999). The prosurvival Bcl-2 homolog Bfl-1/A1 is a direct transcriptional target of NF-kappaB that blocks TNFalpha-induced apoptosis. Genes Dev. *13*, 382–387.